

Multinuclear Complexes Derived from Ferrocenylphosphines and Triruthenium Dodecacarbonyl

Tu Cai Zheng, William R. Cullen,* and Steven J. Rettig

Department of Chemistry, University of British Columbia, 2036 Main Mall,
Vancouver, BC, Canada V6T 1Z1

Received March 24, 1994[®]

Pyrolysis of $\text{Ru}_3(\text{CO})_{11}(\text{PFc}_2\text{Ph})$ in hexanes for 15 h gave the trinuclear cluster $\text{Ru}_3(\text{CO})_8(\mu\text{-CO})(\mu\text{-H})[\mu\text{-}\eta^3\text{-}(\eta^5\text{-C}_5\text{H}_3\text{PFcPh})\text{Fe}(\eta^5\text{-C}_5\text{H}_5)]$ (**11**) in 20% yield. Pyrolysis of $\text{Ru}_3(\text{CO})_{12}$ with PFc_2Ph in octane for 3.5 h gave the tetranuclear cluster $\text{Ru}_4(\text{CO})_{11}(\mu_3\text{-PFc})(\mu\text{-}\eta^1\text{:}\eta^5\text{-C}_5\text{H}_4)$ (**12**) in 12% yield and the previously known **8**, $\text{Ru}_4(\text{CO})_{10}(\mu\text{-CO})\mu_4\text{-PFc}(\mu_4\text{-C}_6\text{H}_4)$, in 10% yield: the mild conditions are noteworthy. Pyrolysis of $\text{Ru}_3(\text{CO})_{12}$ with PET_2Fc in octane for 18 h gave the hexanuclear cluster complexes $\text{Ru}_6\text{C}(\text{CO})_{14}(\mu\text{-PET}_2)_2$ (**13**) and $\text{Ru}_6\text{C}(\text{CO})_{13}(\mu\text{-PET}_2)(\eta^5\text{-C}_5\text{H}_5)$ (**14**) in 15% and 25% yields, respectively, and the pentanuclear derivative $\text{Ru}_5(\text{CO})_9(\mu\text{-CO})(\eta^6\text{-C}_6\text{H}_6)_2(\mu_4\text{-PEt})$ (**15**) (low yield). Pyrolysis of $\text{Ru}_3(\text{CO})_{12}$ with PETFc_2 in toluene for 10 h gave the pentanuclear cluster $\text{Ru}_5(\text{CO})_{12}(\mu_4\text{-PEt})(\eta^6\text{-C}_7\text{H}_8)$ (**16**) in ~5% yield. Crystal data: **8**, monoclinic, space group $P2_1/c$, $a = 14.725(3)$ Å, $b = 9.024(2)$ Å, $c = 22.719(1)$ Å, $\beta = 92.078(8)^\circ$, $Z = 4$; **11**, triclinic, $P\bar{1}$, $a = 12.7671(9)$ Å, $b = 13.284(1)$ Å, $c = 10.2212(8)$ Å, $\alpha = 93.006(6)^\circ$, $\beta = 98.561(6)^\circ$, $\gamma = 83.665(6)^\circ$, $Z = 2$; **12**, monoclinic, space group $P2_1/c$, $a = 10.463(2)$ Å, $b = 16.412(1)$ Å, $c = 17.903(2)$ Å, $\beta = 103.85(1)^\circ$, $Z = 4$; **13**, monoclinic, space group $C2/c$, $a = 12.566(2)$ Å, $b = 16.326(2)$ Å, $c = 17.001(2)$ Å, $\beta = 105.43(1)^\circ$, $Z = 4$; **14**, monoclinic, space group $P2_1/c$, $a = 12.638(2)$ Å, $b = 9.911(3)$ Å, $c = 24.743(5)$ Å, $\beta = 91.33(2)^\circ$, $Z = 4$; **15**, orthorhombic, space group $Cmc2_1$, $a = 16.239(1)$ Å, $b = 13.754(2)$ Å, $c = 11.895(2)$ Å, $Z = 4$; **16**, monoclinic, space group $C2/c$, $a = 31.831(3)$ Å, $b = 9.904(2)$ Å, $c = 17.536(2)$ Å, $\beta = 99.36(1)^\circ$, $Z = 8$. The structures were solved by direct or Patterson methods and were refined by full-matrix least-squares procedures to $R = 0.042, 0.024, 0.027, 0.024, 0.028, 0.032$, and 0.026 for 4943, 8583, 5279, 3650, 6357, 1302, and 5711 reflections with $I \geq 3\sigma(I)$, respectively.

Introduction

Over the past few years, we have focused our attention on the pyrolysis of ferrocenylphosphine derivatives of $\text{Os}_3(\text{CO})_{12}$ in the hope of trapping highly reactive (and previously unknown) organometallic fragments such as ferrocene, $(\text{C}_5\text{H}_3)\text{Fe}(\text{C}_5\text{H}_5)$, and ferrodicyne, $(\text{C}_5\text{H}_3)\text{Fe}(\text{C}_5\text{H}_3)$.^{1–5} We have succeeded in isolating and structurally characterizing the first examples of complexes containing such fragments **1** and **2**.¹ In addition, we also discovered a number of products that showed bonding interactions between the iron atom of the ferrocenyl moiety and an osmium atom, **3–5**.^{2–5} Ferrocenyl (Fc) groups were found to undergo homo- or heteroannular metalation, or both of these reactions, and/or P–C(ferrocenyl) bond cleavage.^{1–6} Some pyrolytic studies involving ferrocenylphosphines and $\text{Ru}_3(\text{CO})_{12}$ and their derivatives have also been described.^{7–9} In particular, pyrolysis of $\text{Ru}_3(\text{CO})_{10}(\text{PFcPh}_2)_2$ led to the

benzynes complex **6** in high yield, but the ferrocenyl moieties remained intact.⁷ Pyrolysis of $\text{Ru}_3(\text{CO})_{10}(\text{Fc}'\text{-}(\text{PPh}_2)_2)$ ($\text{Fc}' = \text{Fe}(\text{C}_5\text{H}_4)_2$) afforded a number of complexes, five of which were characterized by X-ray crystallography.⁸ The formation of the benzynes complexes **7** and **8** involves P–Fc bond cleavage and subsequent formation of one ferrocenyl C–H bond. The most interesting complex **9** contains an ortho:metalated C_5H_3 ring and a weak Fe–Ru bond of $3.097(3)$ Å.⁸ In a similar fashion the pyrolysis of $\text{Ru}_3(\text{CO})_{10}[\text{Fc}'(\text{P}^i\text{Pr}_2)_2]$ afforded mainly three complexes.⁹ Two of the products are derived via β C–H activation and C–P cleavage of the isopropyl groups, while the other complex **10** is derived via one P–Fc' bond cleavage and the formation of an Fe–Ru bond.⁹ Although a structure determination of **10** was not accomplished, the osmium analog, complex **4**, shows a very short Fe–Os bond of $2.813(1)$ Å.² In a continuation of these studies, we wish to report on the preparation and characterization of seven ruthenium cluster complexes derived from ferrocenylphosphines. Six of these structures are new, and one (**8**) is a greatly improved determination of a previously known Ru_4 –benzynes derivative. The original structure of **8** was of limited accuracy.

* To whom correspondence should be addressed.

[®] Abstract published in *Advance ACS Abstracts*, July 15, 1994.

(1) Cullen, W. R.; Rettig, S. J.; Zheng, T. C. *Organometallics* **1992**, *11*, 928.

(2) Cullen, W. R.; Rettig, S. J.; Zheng, T. C. *Organometallics* **1992**, *11*, 277.

(3) Cullen, W. R.; Rettig, S. J.; Zheng, T. C. *Organometallics* **1992**, *11*, 3434.

(4) Cullen, W. R.; Rettig, S. J.; Zheng, T. C. *Can. J. Chem.* **1993**, *71*, 399.

(5) Cullen, W. R.; Rettig, S. J.; Zheng, T. C. *J. Organomet. Chem.* **1993**, *452*, 97.

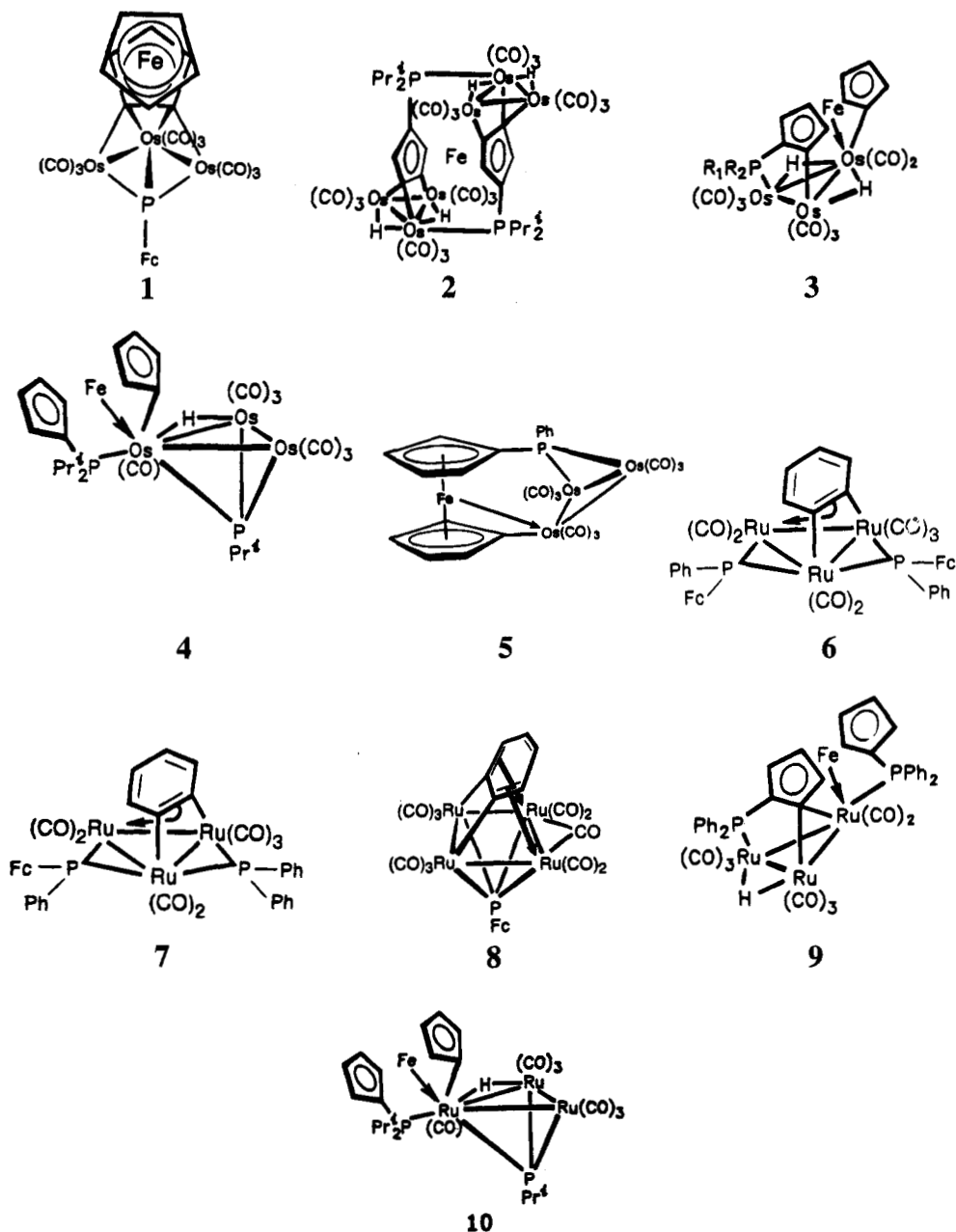
(6) Cullen, W. R.; Rettig, S. J.; Zheng, T. C. *Organometallics* **1993**, *12*, 688.

(7) Cullen, W. R.; Chacon, S. T.; Bruce, M. I.; Einstein, F. W. B.; Jones, R. H. *Organometallics* **1988**, *7*, 2273.

(8) Bruce, M. I.; Cullen, W. R.; Humphrey, P. A.; bin Shawkataly, O.; Snow, M. R.; Tiekink, E. R. T. *Organometallics* **1990**, *9*, 2910.

(9) Cullen, W. R.; Rettig, S. J.; Zheng, T. C. *Organometallics* **1992**, *11*, 853.

Chart 1



Experimental Section

The preparation of the ferrocenylphosphines PFc_2Ph ,^{1,2,10} PEt_2Fc ,⁴ and $PEtFc_2$,^{3,11} have been previously described. The complex $Ru_3(CO)_{11}(PFc_2Ph)$ was prepared as previously reported.¹² All reactions were carried out under an atmosphere of nitrogen, but chromatographic separations were carried out in air, usually on 40 cm \times 6 cm columns. Silica (230–400 mesh) was from Merck, Florisil (60–100 mesh) and alumina (neutral, activity I, 80–200 mesh) were from Fisher Scientific, and the petroleum ether used was the low-boiling fraction (35–60 °C).

³¹P NMR spectra (proton decoupled) were recorded in $CDCl_3$ at ambient temperature with 85% H_3PO_4 as external reference and ¹H NMR spectra in $CDCl_3$ at ambient temperature with

TMS as external reference. A Bruker AC-200E spectrometer was used. Chemical shifts (δ) are given in ppm and couplings (J) in Hz. Fast atom bombardment (FAB) mass spectra were recorded by using an AEI MS-902 spectrometer with 3-nitrobenzyl alcohol as matrix and argon as exciting gas. Elemental analyses were performed by Mr. Peter Borda of this department.

Pyrolysis of $Ru_3(CO)_{11}(PFc_2Ph)$ and Preparation of Complexes 11 and 8. A solution of $Ru_3(CO)_{11}(PFc_2Ph)$ (200 mg, 0.18 mmol) in hexanes (100 mL) was refluxed for 15 h. The solvent was removed in vacuo, and the residue was chromatographed on silica with 2/1 petroleum ether/ CH_2Cl_2 as eluent. The third orange band contained the previously known complex 8 (10%), obtained from the pyrolysis of $Ru_3(CO)_{10}[Fc'(PPh_2)_2]$,⁸ and was identified by TLC, ¹H NMR spectroscopy, mass spectrometry, and analysis. ³¹P NMR (121.4 MHz): δ 408.0. The sixth band contained complex 11, which was obtained as a reddish orange solid (20%). ³¹P NMR (121.4 MHz): δ 24.6. ¹H NMR (300 MHz): δ 8.0 (m, 2H), 7.5 (m, 3H), 5.5 (m, 2H), 4.5 (s, 5H), 4.4–4.2 (m, 3H), 4.0 (s, 5H), 3.6 (m, 1H), 3.0 (m, 1H), –15.0 (d, 1H, $J = 28.1$). Mass

(10) Chacon, S. T. M.Sc. Thesis, The University of British Columbia, 1986.

(11) Zheng, T. C. Ph.D. Thesis, The University of British Columbia, 1993.

(12) Chacon, S. T.; Cullen, W. R.; Bruce, M. I.; bin Shawkataly, O.; Einstein, F. W. B.; Jones, R. H.; Willis, A. C. *Can. J. Chem.* **1990**, *68*, 2001.

Table 1. Crystallographic Data^a

	8	11	12	13	14	15	16
formula	C ₂₇ H ₁₃ FeO ₁₁ PRu ₄	C ₃₅ H ₂₃ Fe ₂ O ₉ PRu ₃	C ₂₆ H ₁₃ FeO ₁₁ PRu ₄	C ₂₃ H ₂₀ O ₁₄ P ₂ Ru ₆	C ₂₃ H ₁₅ O ₁₃ PRu ₆	C ₂₂ H ₁₅ FeO ₁₀ PRu ₅	C ₂₁ H ₁₃ O ₁₂ PRu ₅
fw	1004.49	1033.44	992.48	1188.77	1136.76	975.68	993.65
color, habit	red, plate	black, plate	red, prism	red, prism	red, prism	dark red, plate	dark green, plate
cryst syst	monoclinic	triclinic	monoclinic	monoclinic	monoclinic	orthorhombic	monoclinic
space group	<i>P</i> 2 ₁ / <i>c</i>	<i>P</i> $\bar{1}$	<i>P</i> 2 ₁ / <i>c</i>	<i>C</i> 2/ <i>c</i>	<i>P</i> 2 ₁ / <i>c</i>	<i>C</i> mc2 ₁	<i>C</i> 2/ <i>c</i>
<i>a</i> , Å	14.725(3)	12.7671(9)	10.463(2)	12.566(2)	12.638(2)	16.239(1)	31.831(3)
<i>b</i> , Å	9.024(2)	13.284(1)	16.412(1)	16.326(2)	9.911(3)	13.754(2)	9.904(2)
<i>c</i> , Å	22.719(1)	10.2212(8)	17.903(2)	17.001(2)	24.743(5)	11.895(2)	17.536(2)
α , deg	90	93.006(6)	90	90	90	90	90
β , deg	92.078(8)	98.561(6)	103.85(1)	105.43(1)	91.33(2)	90	99.36(1)
γ , deg	90	83.665(6)	90	90	90	90	90
<i>V</i> , Å ³	3017.0(7)	1702.6(2)	2985.1(6)	3362.2(8)	3098.5(10)	2656.8(5)	5455(1)
<i>Z</i>	4	2	4	4	4	4	8
ρ_{calc} , g/cm ³	2.211	2.016	2.208	2.348	2.437	2.439	2.420
<i>F</i> (000)	1920	1008	1896	2256	2144	1848	3760
μ (Mo K α), cm ⁻¹	25.37	22.34	25.25	27.84	29.63	28.91	27.72
cryst size, mm	0.05 × 0.25 × 0.35	0.08 × 0.30 × 0.38	0.12 × 0.20 × 0.35	0.12 × 0.15 × 0.25	0.15 × 0.25 × 0.30	0.04 × 0.20 × 0.25	0.04 × 0.20 × 0.45
transmissn factors	0.75–1.00	0.61–1.00	0.87–1.00	0.82–1.00	0.87–1.00	0.50–1.00	0.68–1.00
scan type	ω -2 θ	ω -2 θ	ω -2 θ	ω -2 θ	ω	ω -2 θ	ω -2 θ
scan range, ω , deg	1.20 + 0.35	1.31 + 0.35	1.26 + 0.35	1.52 + 0.35	0.88 + 0.35	1.21 + 0.35	1.05 + 0.35
	tan θ	tan θ	tan θ	tan θ	tan θ	tan θ	tan θ
scan rate, deg min ⁻¹	32	32	16	32	32	16	16
data collected	+ <i>h</i> ,+ <i>k</i> ,± <i>l</i>	+ <i>h</i> ,± <i>k</i> ,± <i>l</i>	+ <i>h</i> ,+ <i>k</i> ,± <i>l</i>	+ <i>h</i> ,+ <i>k</i> ,± <i>l</i>	+ <i>h</i> ,+ <i>k</i> ,± <i>l</i>	+ <i>h</i> ,+ <i>k</i> ,+ <i>l</i>	+ <i>h</i> ,+ <i>k</i> ,± <i>l</i>
2 θ_{max} , deg	60	65	60	65	65	60	65
cryst decay, %	negligible	negligible	negligible	negligible	negligible	negligible	negligible
total no. of rflns	9662	12 800	9428	6511	12 219	2172	10 507
no. of unique rflns	9321	12 314	8979	6263	11 771	2172	10 339
<i>R</i> _{merge}	0.041	0.019	0.0281	0.020	0.024	0.024	0.030
no. of rflns with <i>I</i> ≥ 3 σ (<i>I</i>)	4943	8583	5279	3650	6357	1302	5711
no. of variables	397	456	389	205	388	186	352
<i>R</i>	0.042	0.024	0.027	0.024	0.028	0.032	0.026
<i>R</i> _w	0.044	0.026	0.026	0.023	0.025	0.032	0.024
GOF	2.03	1.49	1.50	1.31	1.37	1.47	1.32
max Δ / σ (final cycle)	0.0009	0.01	0.06	0.001	0.001	0.03	0.004
residual density, e/Å ³	-1.17 to +1.31	-0.41 to +0.43	-0.44 to +0.47	-0.43 to +0.50	-0.52 to +0.74	-0.58 to +0.58	-0.46 to +0.47

^a Conditions: temperature 294 K; Rigaku AFC6S diffractometer; Mo K α ($\lambda = 0.710 69$ Å) radiation; graphite monochromator; takeoff angle 6.0°; aperture 6.0 × 6.0 mm at a distance of 285 mm from the crystal; stationary background counts at each end of the scan (scan/background time ratio 2:1); $\sigma^2(F^2) = [S^2(C + 4B)]/(L_p)^2$ (*S* = scan rate, *C* = scan count, *B* = normalized background count); function minimized $\sum w(|F_o| - |F_c|)^2$, where $w = 4F_o^2/\sigma^2(F_o^2)$; $R = \sum(|F_o| - |F_c|)/\sum|F_o|$; $R_w = (\sum w(|F_o| - |F_c|)^2/\sum w|F_o|^2)^{1/2}$; GOF = $[\sum w(|F_o| - |F_c|)^2/(m - n)]^{1/2}$. Values given for *R*, *R*_w, and GOF are based on those reflections with *I* ≥ 3 σ (*I*).

spectrum (FAB): *m/e* 1035 (P⁺), 1007, 979, 950, 922, 893, 864, 838 (base peak), 809, 776. Anal. Calcd for C₃₅H₂₃Fe₂O₉PRu₃: C, 40.68; H, 2.24. Found: C, 40.78; H, 2.30. Suitable crystals of **11** were obtained from 2/1 hexanes/CH₂Cl₂ solutions.

Pyrolysis of Ru₃(CO)₁₂ with PFc₂Ph and Preparation of Complexes **12 and **8**.** A solution of Ru₃(CO)₁₂ (256 mg, 0.40 mmol) and PFc₂Ph (190 mg, 0.40 mmol) in octane (50 mL) was refluxed for 3.5 h. ¹H NMR spectroscopy showed the absence of any hydrides. The reaction solvent was removed in vacuo, and the residue was chromatographed on alumina with 4/1 petroleum ether/CH₂Cl₂ as eluent. The second band contained complex **12**, which was obtained as a red solid (12%). ³¹P NMR (121.4 MHz): δ 418.0. ¹H NMR (300 MHz): δ 5.28 (m, 1H), 5.18 (m, 1H), 4.80 (m, 1H), 4.54 (m, 2H), 4.50 (m, 1H), 4.44 (m, 1H), 4.35 (m, 1H), 4.31 (s, 5H). Mass spectrum (FAB): *m/e* 993 (P⁺), 966, 935, 909 (base peak), 880, 853, 826, 797, 768, 741, 683. Anal. Calcd for C₂₆H₁₃FeO₁₁PRu₄: C, 31.47; H, 1.32. Found: C, 31.61; H, 1.38. Crystals of **12** suitable for an X-ray diffraction study were obtained from 5/1 hexane/CH₂Cl₂ solutions. The third orange band contained **8** (20%), which was identified by TLC and ¹H and ³¹P NMR spectroscopy. Crystals were obtained from the same solvent mixture.

Pyrolysis of Ru₃(CO)₁₂ with PEt₂Fc and Preparation of Complexes **13–**15**.** Triruthenium dodecacarbonyl (200 mg, 0.31 mmol) and PEt₂Fc (75 mg, 0.27 mmol) in octane was refluxed for 18 h. TLC revealed the formation of more than 10 products. The solvent was removed in vacuo, and the residue was chromatographed on Florisil with 4/1 petroleum ether/CH₂Cl₂ as eluent. The first yellow band contained

ferrocene (2%), identified by TLC and ¹H NMR spectroscopy. The third band and first major one contained complex **13**, which was obtained as an orange solid (15%). The fourth band contained complex **14**, which was obtained as a brownish red solid (25%). The fifth band (~10%) contained a mixture of at least three complexes as judged by TLC. Slow evaporation of the eluent from the column fraction gave a few crystals of the pure product **15**. Crystals of **13** and **14** were similarly obtained.

13: ³¹P NMR (81.0 MHz) δ 370.4; ¹H NMR (200 MHz) δ 2.34 (m), 2.12 (m), 1.33 (m), 1.26 (m); mass spectrum (FAB) *m/e* 1189 (P⁺, base peak), 1159, 1133, 1025, 1077, 1046, 1017, 991, 963, 935, 906.

14: ³¹P NMR (81.0 MHz) δ 366.8; ¹H NMR (200 MHz) δ 4.62 (s, 5H), 2.23 (m, 2H), 2.04 (m, 2H), 1.40–1.15 (m, 6H); mass spectrum (FAB) *m/e* 1137 (P⁺, base peak), 1109, 1080, 1052, 1024, 995, 964, 935, 907, 879.

Pyrolysis of Ru₃(CO)₁₂ with PEt₂Fc and Preparation of Complex **16.** A solution of Ru₃(CO)₁₂ (150 mg, 0.23 mmol) and PEt₂Fc (110 mg, 0.26 mmol) in toluene (40 mL) was refluxed for 10 h. TLC revealed the presence of more than 10 products. The solvent was removed in vacuo, and the residue was chromatographed on silica with 4/1 petroleum ether/CH₂Cl₂ as eluent. The second band contained complex **16**, which was obtained as a dark green solid (~5%). ³¹P NMR (81.0 MHz): δ 425.1. Mass spectrum (FAB): *m/e* 995 (P⁺, base peak), 967, 938, 910, 882, 854, 826, 798, 770, 742. Anal. Calcd for C₂₁H₁₃O₁₂PRu₅: C, 25.38; H, 1.32. Found: 25.57; H, 1.41.

X-ray Crystallographic Analyses of **8 and **11**–**16**.** Crystallographic data appear in Table 1. The final unit-cell

Table 2. Final Atomic Coordinates (Fractional) and B_{eq} Values for 11

atom	x	y	z	$B_{\text{eq}}, \text{\AA}^2$
Ru(1)	0.21611(2)	0.06989(1)	0.39459(2)	2.399(4)
Ru(2)	0.28771(2)	0.27656(2)	0.47970(2)	2.524(4)
Ru(3)	0.06755(2)	0.23567(1)	0.42694(2)	2.422(4)
Fe(1)	0.20939(3)	0.07470(2)	0.10164(3)	2.182(6)
Fe(2)	0.53414(3)	0.34334(3)	0.17850(3)	2.554(7)
P(1)	0.27609(4)	0.30758(4)	0.25057(5)	1.973(10)
O(1)	0.1115(2)	0.0684(2)	0.6342(2)	4.67(5)
O(2)	0.1140(2)	-0.1216(2)	0.3144(2)	5.13(6)
O(3)	0.3941(2)	-0.0560(2)	0.5541(3)	9.41(10)
O(4)	0.1815(2)	0.4863(2)	0.5486(3)	6.05(6)
O(5)	0.5232(2)	0.2989(2)	0.5641(2)	5.25(6)
O(6)	0.2919(2)	0.2061(2)	0.7596(2)	7.42(8)
O(7)	-0.1531(2)	0.1650(2)	0.3587(3)	5.56(6)
O(8)	-0.0091(2)	0.4337(2)	0.2845(2)	5.22(6)
O(9)	0.0277(2)	0.3237(2)	0.6978(2)	6.24(7)
C(1)	0.1829(2)	0.2257(2)	0.1644(2)	1.99(4)
C(2)	0.1197(2)	0.1692(2)	0.2373(2)	2.15(4)
C(3)	0.0527(2)	0.1174(2)	0.1348(2)	2.59(4)
C(4)	0.0681(2)	0.1454(2)	0.0083(2)	2.78(5)
C(5)	0.1495(2)	0.2118(2)	0.0255(2)	2.50(4)
C(6)	0.3658(2)	0.0044(2)	0.1277(3)	3.29(5)
C(7)	0.2965(2)	-0.0694(2)	0.1395(3)	3.31(5)
C(8)	0.2243(2)	-0.0728(2)	0.0232(3)	3.46(6)
C(9)	0.2496(2)	-0.0028(2)	-0.0641(2)	3.68(6)
C(10)	0.3385(2)	0.0443(2)	0.0019(3)	3.46(6)
C(11)	0.3941(2)	0.2792(2)	0.1728(2)	2.10(4)
C(12)	0.4836(2)	0.2093(2)	0.2160(2)	2.72(5)
C(13)	0.5496(2)	0.1957(2)	0.1152(3)	3.58(6)
C(14)	0.5021(2)	0.2573(2)	0.0089(3)	3.52(6)
C(15)	0.4061(2)	0.3095(2)	0.0432(2)	2.65(5)
C(16)	0.5571(3)	0.4511(2)	0.3269(3)	4.24(7)
C(17)	0.6455(2)	0.3777(2)	0.3343(3)	4.08(7)
C(18)	0.6886(2)	0.3765(2)	0.2155(3)	4.37(7)
C(19)	0.6267(2)	0.4498(2)	0.1338(3)	4.23(7)
C(20)	0.5452(3)	0.4960(2)	0.2024(3)	4.35(7)
C(21)	0.2312(2)	0.4371(2)	0.1975(2)	2.46(4)
C(22)	0.1604(2)	0.4594(2)	0.0842(3)	3.25(5)
C(23)	0.1326(2)	0.5597(2)	0.0482(3)	4.31(7)
C(24)	0.1751(3)	0.6370(2)	0.1246(4)	4.77(8)
C(25)	0.2458(3)	0.6163(2)	0.2356(4)	4.85(8)
C(26)	0.2742(2)	0.5169(2)	0.2728(3)	3.62(6)
C(27)	0.1277(2)	0.1035(2)	0.5366(2)	3.20(5)
C(28)	0.1498(2)	-0.0476(2)	0.3432(3)	3.30(6)
C(29)	0.3261(3)	-0.0099(2)	0.4928(3)	4.62(7)
C(30)	0.2219(2)	0.4090(2)	0.5232(3)	3.91(6)
C(31)	0.4364(2)	0.2922(2)	0.5233(2)	3.40(6)
C(32)	0.2876(3)	0.2314(3)	0.6544(3)	4.37(7)
C(33)	-0.0702(2)	0.1889(2)	0.3837(3)	3.39(6)
C(34)	0.0242(2)	0.3602(2)	0.3335(3)	3.14(5)
C(35)	0.0406(2)	0.2934(2)	0.5953(3)	3.88(6)

$$^a B_{\text{eq}} = \frac{8}{3}\pi^2(U_{11}(aa^*)^2 + U_{22}(bb^*)^2 + 2U_{12}aa^*bb^* \cos \gamma + 2U_{13}aa^*cc^* \cos \beta + 2U_{23}bb^*cc^* \cos \alpha).$$

parameters were obtained by least squares on the setting angles for 25 reflections with $2\theta = 35.4\text{--}42.6^\circ$ for **8**, $45.3\text{--}49.4^\circ$ for **11**, $25.3\text{--}33.0^\circ$ for **12**, $43.5\text{--}51.7^\circ$ for **13**, $42.9\text{--}46.7^\circ$ for **14**, $21.5\text{--}33.4^\circ$ for **15**, and $35.0\text{--}41.5^\circ$ for **16**. The intensities of 3 standard reflections, measured every 200 reflections throughout the data collections, showed only small random fluctuations for all seven complexes. The data were processed¹³ and corrected for Lorentz and polarization effects and absorption (empirical, based on azimuthal scans for three reflections).

The structures were solved by direct (**8**, **11**, **13**, **14**, and **15**) or Patterson (**12** and **16**) methods. The structure analyses of **11**, **13**, **15**, and **16**, where there was a choice between centrosymmetric and noncentrosymmetric space groups, were initiated in the centrosymmetric space groups on the basis of the E statistics and Patterson functions. These choices were confirmed by subsequent calculations. Complex **13** has exact

Table 3. Final Atomic Coordinates (Fractional) and B_{eq} Values for 12

atom	x	y	z	$B_{\text{eq}}, \text{\AA}^2$
Ru(1)	0.53865(3)	0.53355(2)	0.25106(2)	2.65(1)
Ru(2)	0.28173(3)	0.63454(2)	0.33815(2)	2.59(1)
Ru(3)	0.32427(3)	0.56438(2)	0.11815(2)	2.85(1)
Ru(4)	0.26333(3)	0.48765(2)	0.24415(2)	2.70(1)
Fe(1)	-0.01401(6)	0.75521(4)	0.09132(4)	3.80(3)
P(1)	0.21897(10)	0.62595(6)	0.20393(6)	2.56(4)
O(1)	0.5664(4)	0.3559(2)	0.2929(2)	5.8(2)
O(2)	0.6819(3)	0.5044(2)	0.1259(2)	5.3(2)
O(3)	0.3094(4)	0.8156(2)	0.3678(3)	7.6(2)
O(4)	0.3688(4)	0.5843(3)	0.5075(2)	6.2(2)
O(5)	-0.0072(3)	0.6108(3)	0.3439(2)	6.1(2)
O(6)	0.0994(3)	0.5708(2)	-0.0234(2)	5.7(2)
O(7)	0.4722(4)	0.7031(2)	0.0640(2)	6.1(2)
O(8)	0.4169(4)	0.4182(2)	0.0376(2)	6.2(2)
O(9)	-0.0261(3)	0.4571(2)	0.2267(2)	6.7(2)
O(10)	0.2806(4)	0.3319(2)	0.1543(2)	7.1(2)
O(11)	0.3407(3)	0.4151(2)	0.4055(2)	5.5(2)
C(1)	0.4762(4)	0.6265(2)	0.3287(2)	2.9(2)
C(2)	0.5373(4)	0.6680(2)	0.2760(2)	3.2(2)
C(3)	0.6697(4)	0.6403(3)	0.2870(3)	3.6(2)
C(4)	0.6937(4)	0.5829(3)	0.3462(3)	3.8(2)
C(5)	0.5764(4)	0.5744(2)	0.3721(2)	3.1(2)
C(6)	0.0531(4)	0.6657(2)	0.1710(2)	3.0(2)
C(7)	0.0032(5)	0.7343(3)	0.2046(3)	4.2(2)
C(8)	-0.1311(5)	0.7457(3)	0.1671(3)	4.6(2)
C(9)	-0.1646(4)	0.6860(3)	0.1105(3)	4.5(2)
C(10)	-0.0542(4)	0.6370(3)	0.1117(2)	3.6(2)
C(11)	0.1282(9)	0.7895(7)	0.0388(8)	11.8(7)
C(12)	0.0936(9)	0.8555(5)	0.0795(5)	9.2(4)
C(13)	-0.0401(8)	0.8706(4)	0.0485(6)	8.3(4)
C(14)	-0.0831(8)	0.8139(7)	-0.0077(5)	9.9(5)
C(15)	0.022(2)	0.7658(6)	-0.0134(6)	12.5(7)
C(16)	0.5484(4)	0.4216(3)	0.2739(3)	4.0(2)
C(17)	0.6211(4)	0.5137(3)	0.1701(3)	3.8(2)
C(18)	0.2993(5)	0.7476(3)	0.3572(3)	4.2(2)
C(19)	0.3379(4)	0.6015(3)	0.4447(3)	3.9(2)
C(20)	0.0976(4)	0.6234(3)	0.3417(2)	3.7(2)
C(21)	0.1796(5)	0.5720(3)	0.0318(3)	3.9(2)
C(22)	0.4183(4)	0.6502(3)	0.0824(2)	3.8(2)
C(23)	0.3858(5)	0.4719(3)	0.0694(3)	4.2(2)
C(24)	0.0827(4)	0.4694(3)	0.2339(3)	4.2(2)
C(25)	0.2794(5)	0.3926(3)	0.1848(3)	4.4(2)
C(26)	0.3103(4)	0.4462(3)	0.3465(3)	3.7(2)

$$^a B_{\text{eq}} = \frac{8}{3}\pi^2 \sum \sum U_{ij} a_i^* a_j^* (a_i a_j).$$

(crystallographic) C_2 symmetry, the axis passing through the central carbide carbon atom.

All non-hydrogen atoms were refined with anisotropic thermal parameters. The metal hydride atom in **11** was refined with an isotropic thermal parameter. The remaining hydrogen atoms were fixed in calculated positions ($\text{C-H} = 0.99 \text{ \AA}$ for **8**, **11**, **13**, **14**, and **15** and 0.98 \AA for **12** and **16**; $B_{\text{H}} = 1.2B_{\text{bonded atom}}$). Secondary extinction corrections were applied for **11**–**13**, the final values of the extinction coefficients being $[4.8(2)] \times 10^{-7}$, $[5.6(2)] \times 10^{-8}$, and $[1.67(8)] \times 10^{-7}$, respectively. Neutral atom scattering factors for all atoms^{14a} and anomalous dispersion corrections for the non-hydrogen atoms^{14b} were taken from ref 14. Final atomic coordinates and equivalent isotropic thermal parameters and selected bond lengths and bond angles appear in Tables 2–10. Hydrogen atom parameters, anisotropic thermal parameters, bond lengths, bond angles, torsion angles, intermolecular contacts, and least-squares planes for the structures are included as supplementary material.

Results and Discussion

Pyrolysis of Ru₃(CO)₁₁(PF₂Ph). Pyrolysis of Ru₃(CO)₁₁(PF₂Ph) in hexanes for 15 h gives **11** in 20%

(13) teXsan Crystal Structure Analysis Package; Molecular Structure Corp., 1985 and 1992.

(14) (a) *International Tables for X-Ray Crystallography*; Kynoch Press: Birmingham, England, 1974; Vol. IV, pp 99–102. (b) *International Tables for X-Ray Crystallography*; Kluwer Academic: Boston, MA, 1992; Vol. C, pp 200–206.

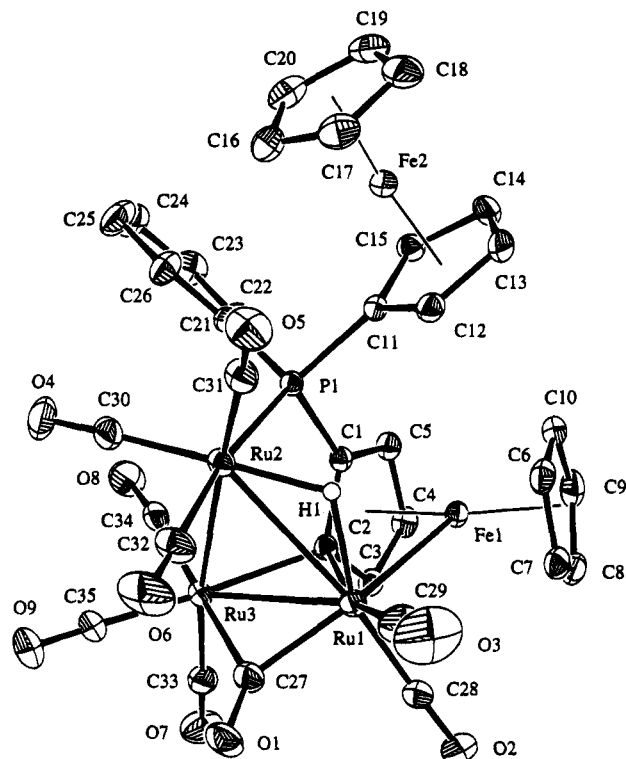


Figure 1. ORTEP diagram for **11** (33% probability thermal ellipsoids).

Table 4. Final Atomic Coordinates (Fractional) and B_{eq} Values for **13**

atom	x	y	z	$B_{eq}, \text{\AA}^2$
Ru(1)	0.12216(2)	0.17919(2)	0.27657(2)	2.355(5)
Ru(2)	0.01166(2)	0.26371(2)	0.13239(1)	2.435(5)
Ru(3)	0.11765(2)	0.35695(2)	0.27744(2)	2.652(6)
P(1)	0.15342(7)	0.17344(5)	0.15011(5)	2.80(2)
O(1)	0.1199(3)	-0.0022(2)	0.3083(2)	5.82(8)
O(2)	0.3518(2)	0.1772(2)	0.3897(2)	5.19(7)
O(3)	0.0913(3)	0.3772(2)	0.0185(2)	6.04(9)
O(4)	-0.1465(2)	0.1690(2)	-0.0021(2)	5.41(8)
O(5)	0.1085(3)	0.5112(2)	0.1765(2)	6.26(9)
O(6)	0.1482(2)	0.4446(2)	0.4399(2)	5.20(8)
O(7)	0.3672(2)	0.3470(2)	0.3075(2)	6.10(9)
C(1)	0.1183(3)	0.0663(2)	0.2946(2)	3.56(8)
C(2)	0.2663(3)	0.1787(2)	0.3460(2)	3.35(8)
C(3)	0.0604(3)	0.3352(2)	0.0609(2)	3.83(9)
C(4)	-0.0893(3)	0.2045(2)	0.0498(2)	3.49(8)
C(5)	0.1116(3)	0.4532(2)	0.2140(2)	3.93(9)
C(6)	0.1316(3)	0.4062(2)	0.3826(2)	3.61(8)
C(7)	0.2737(3)	0.3483(2)	0.2966(2)	3.86(9)
C(8)	0.0000	0.2669(3)	0.2500	2.25(8)
C(9)	0.2818(3)	0.2114(3)	0.1319(2)	4.30(9)
C(10)	0.3810(4)	0.1594(4)	0.1658(3)	6.6(1)
C(11)	0.1310(3)	0.0742(2)	0.0978(2)	4.07(9)
C(12)	0.1257(4)	0.0778(3)	0.0069(3)	5.9(1)

$$^a B_{eq} = \frac{8}{3}\pi^2(U_{11}(aa^*)^2 + U_{22}(bb^*)^2 + U_{33}(cc^*)^2 + 2U_{12}aa^*bb^* \cos \gamma + 2U_{13}aa^*cc^* \cos \beta + 2U_{23}bb^*cc^* \cos \alpha).$$

yield. This complex shows a ^{31}P NMR resonance at 24.6 ppm, suggesting the presence of a phosphine. The ^1H NMR spectrum shows the presence of a phenyl group, 17 ferrocenyl protons with two C_5H_5 rings, and a hydride. The mass spectrum gives the parent ion at m/e 1035, corresponding to the loss of two CO groups from the starting material. The structure of this complex was established by an X-ray crystallographic study. An ORTEP diagram of the molecule with 33% probability thermal ellipsoids is shown in Figure 1.

The structure of **11** consists of a closed Ru_3 metal framework with a face-capping and significantly modi-

Table 5. Final Atomic Coordinates (Fractional) and B_{eq} Values for **14**

atom	x	y	z	$B_{eq}, \text{\AA}^2$
Ru(1)	0.14378(2)	0.13394(3)	0.38209(1)	2.612(7)
Ru(2)	0.36071(2)	0.43213(3)	0.39177(1)	2.676(7)
Ru(3)	0.34707(2)	0.17962(3)	0.33496(1)	2.524(7)
Ru(4)	0.18244(2)	0.37354(3)	0.32086(1)	2.462(6)
Ru(5)	0.15653(3)	0.38877(3)	0.43813(1)	2.674(7)
Ru(6)	0.32125(3)	0.19192(3)	0.45346(1)	2.706(7)
P(1)	0.26982(8)	0.2556(1)	0.25622(4)	2.88(2)
O(1)	0.3191(3)	0.7059(4)	0.4416(2)	6.4(1)
O(2)	0.4674(3)	0.5721(4)	0.2993(1)	6.1(1)
O(3)	0.5716(3)	0.3892(4)	0.4492(2)	7.4(1)
O(4)	0.5746(2)	0.2322(4)	0.3065(1)	5.71(10)
O(5)	0.3649(3)	-0.1194(4)	0.3123(2)	6.4(1)
O(6)	0.2031(3)	0.6532(3)	0.2734(2)	6.0(1)
O(7)	-0.0416(2)	0.3373(4)	0.2804(1)	5.62(10)
O(8)	0.1970(3)	0.5281(5)	0.5459(1)	7.1(1)
O(9)	-0.0282(3)	0.2458(4)	0.4873(1)	6.1(1)
O(10)	0.0149(3)	0.6111(4)	0.3924(1)	5.59(10)
O(11)	0.4069(3)	0.3009(4)	0.5605(1)	6.0(1)
O(12)	0.2093(3)	-0.0261(4)	0.5150(1)	6.7(1)
O(13)	0.5138(3)	0.0151(4)	0.4358(1)	7.3(1)
C(1)	0.1064(3)	-0.0523(5)	0.3367(2)	4.0(1)
C(2)	0.1125(4)	-0.0799(4)	0.3927(2)	4.3(1)
C(3)	0.0345(4)	-0.0053(5)	0.4184(2)	4.5(1)
C(4)	-0.0215(3)	0.0702(5)	0.3791(2)	4.4(1)
C(5)	0.0227(3)	0.0425(5)	0.3284(2)	3.7(1)
C(6)	0.2477(3)	0.2768(4)	0.3969(1)	2.15(7)
C(7)	0.3284(4)	0.5998(5)	0.4253(2)	4.2(1)
C(8)	0.4260(3)	0.5185(5)	0.3334(2)	4.0(1)
C(9)	0.4908(4)	0.4008(5)	0.4291(2)	4.5(1)
C(10)	0.4896(3)	0.2130(5)	0.3168(2)	3.50(10)
C(11)	0.3555(3)	-0.0064(5)	0.3193(2)	3.7(1)
C(12)	0.1964(3)	0.5477(5)	0.2911(2)	3.7(1)
C(13)	0.0440(3)	0.3474(4)	0.2947(2)	3.51(10)
C(14)	0.1838(3)	0.4772(5)	0.5054(2)	4.2(1)
C(15)	0.0421(4)	0.2905(5)	0.4653(2)	4.3(1)
C(16)	0.0705(3)	0.5277(5)	0.4064(2)	3.7(1)
C(17)	0.3764(4)	0.2630(5)	0.5204(2)	4.0(1)
C(18)	0.2470(4)	0.0537(5)	0.4893(2)	4.4(1)
C(19)	0.4408(4)	0.0817(5)	0.4379(2)	4.4(1)
C(20)	0.1924(3)	0.1386(5)	0.2143(2)	4.0(1)
C(21)	0.2580(4)	0.0399(6)	0.1806(2)	5.9(1)
C(22)	0.3481(3)	0.3448(5)	0.2065(2)	4.0(1)
C(23)	0.2836(4)	0.4160(6)	0.1628(2)	5.8(1)

$$^a B_{eq} = \frac{8}{3}\pi^2(U_{11}(aa^*)^2 + U_{22}(bb^*)^2 + U_{33}(cc^*)^2 + 2U_{12}aa^*bb^* \cos \gamma + 2U_{13}aa^*cc^* \cos \beta + 2U_{23}bb^*cc^* \cos \alpha).$$

fied ferrocenylphosphine ligand, eight terminal carbonyls, a bridging carbonyl, and a bridging hydride which was located in the structure refinement. The cluster is electron precise, since an iron–ruthenium bond is present. The Ru–Ru bond distances span a large range, with Ru(1)–Ru(3) being the shortest at 2.7817(6) Å, Ru(1)–Ru(2) being very long at 3.0316(7) Å, and Ru(2)–Ru(3) being of intermediate length 2.885(1) Å, which is comparable to that in $\text{Ru}_3(\text{CO})_{12}$ (2.854(4) Å).¹⁵ The shortest Ru–Ru bond is bridged asymmetrically by carbonyl C(27) (Ru(1)–C(27) = 1.971(3) Å, Ru(3)–C(27) = 2.140(3) Å) and symmetrically by the ortho-metalated ferrocenyl carbon atom C(2) (Ru(1)–C(2) = 2.260(2) Å, Ru(3)–C(2) = 2.248(2) Å). Such symmetrical bridging of an ortho-metalated aryl moiety is present in the complex, $\text{Os}_3(\text{CO})_8(\text{H})[\text{Ph}_2\text{PCH}_2\text{P}(\text{Ph})\text{C}_6\text{H}_4]$ (**17**),¹⁶ but this compound is coordinatively unsaturated and undergoes a facile reversible addition reaction with CO.^{17,18} The longest Ru(1)–Ru(2) bond is, as expected, bridged by the hydride.

(15) Churchill, M. R.; Hollander, F. J.; Hutchinson, J. P. *Inorg. Chem.* **1977**, *16*, 2655.

(16) Clucas, J. A.; Foster, D. F.; Harding, M. M.; Smith, A. K. J. *Chem. Soc., Chem. Commun.* **1984**, 949.

Table 6. Final Atomic Coordinates (Fractional) and B_{eq} Values for 15

atom	x	y	z	B _{eq} , ^a Å ²	occ
Ru(1)	0.41493(5)	0.34117(5)	0.50560	2.86(2)	
Ru(2)	0.41083(5)	0.13650(6)	0.49140(10)	3.07(2)	
Ru(3)	0.5000	0.22573(9)	0.66684(14)	2.71(2)	0.5
P(1)	0.5000	0.2483(3)	0.3958(4)	2.90(8)	0.5
O(1)	0.5000	0.4609(8)	0.6823(12)	4.3(3)	0.5
O(2)	0.4091(5)	-0.0808(7)	0.5288(14)	9.0(4)	
O(3)	0.3135(7)	0.0975(10)	0.2799(9)	7.8(3)	
O(4)	0.2606(6)	0.1651(7)	0.6352(11)	7.5(3)	
O(5)	0.5000	0.0158(12)	0.746(2)	6.9(4)	0.5
O(6)	0.3655(7)	0.2889(8)	0.8281(10)	7.1(3)	
C(1)	0.5000	0.4009(12)	0.615(2)	3.5(4)	0.5
C(2)	0.4143(6)	0.0000(9)	0.5179(15)	5.2(3)	
C(3)	0.3493(8)	0.1141(10)	0.3575(12)	4.7(3)	
C(4)	0.3173(9)	0.1565(10)	0.5802(14)	5.4(4)	
C(5)	0.5000	0.0925(12)	0.709(2)	4.3(4)	0.5
C(6)	0.4148(8)	0.2654(10)	0.7665(11)	4.6(3)	
C(7)	0.2826(9)	0.3739(13)	0.516(2)	7.3(5)	
C(8)	0.3222(9)	0.4468(13)	0.5740(14)	5.5(4)	
C(9)	0.3680(9)	0.4922(9)	0.506(2)	7.0(4)	
C(10)	0.3674(10)	0.4510(14)	0.389(2)	7.1(5)	
C(11)	0.3040(11)	0.3710(14)	0.406(2)	7.0(5)	
C(12)	0.5000	0.248(2)	0.243(2)	7.4(8)	0.5
C(13)	0.454(3)	0.298(3)	0.176(6)	13(1)	0.5

^a B_{eq} = $\frac{8}{3}\pi^2(U_{11}(aa^*)^2 + U_{22}(bb^*)^2 + 2U_{12}aa^*bb^* \cos \gamma + 2U_{13}aa^*cc^* \cos \beta + 2U_{23}bb^*cc^* \cos \alpha)$.

The presence of both the dangling ferrocenyl group (Fc(2): Cp(3), Cp(4)) and the significantly modified ferrocenyl moiety (Fc(1): Cp(1), Cp(2)) in the same molecule invites comparison. In Fc(2), all Fe—C bonds are the same (average 2.042 Å) and normal; this is also reflected by normal Fe(2)—Cp(3) and Fe(2)—Cp(4) distances (1.64 and 1.66 Å, respectively). In Cp(1), the Fe(1)—C(2) bond is very long at 2.186(2) Å, the Fe(1)—C(1) and Fe(1)—C(3) bonds (average 2.085 Å) are slightly lengthened, and the Fe(1)—C(4) and Fe(1)—C(5) bonds are normal (average 2.051 Å). In Cp(2), Fe(1)—C(6) and Fe(1)—C(7) (average 2.110 Å) are longer than the other three (average 2.057 Å). The Fe(1)—Cp bonds (both 1.70 Å) are also longer than those of Fc(2) by ca. 0.05 Å. In the Cp(3) and Cp(4) rings, all C—C bonds are effectively the same and normal (average 1.415 Å). In the Cp(1) ring, however, the C(1)—C(2) bond is significantly lengthened to 1.462(3) Å and C(2)—C(3) (1.444(3) Å) perhaps slightly lengthened; the other three (average 1.419 Å) are normal. The P(1)—C(11)—C(12) and P(1)—C(11)—C(15) angles (126.5(2) and 125.3(2)°) are the same and ideal, but the P(1)—C(1)—C(2) (120.8(1)°) and P(1)—C(1)—C(5) angles (129.5(2)°) differ by ca. 10°. This is probably the result of the metalation, since such differences were not found in Os₃(CO)₁₀(PF₂Ph)₂.¹⁹

The Cp(3) and Cp(4) rings have a ring tilt angle of 6.3°, while the Cp(1) and Cp(2) rings have opened up considerably to an angle of 21.1°, which is similar to that found in Ru₃(CO)₈(H)[(C₅H₄PPh₂)Fe(C₅H₃PPh₂)] (9).⁸

The C(2)—Ru(1) and C(2)—Ru(3) bonds are slightly longer than typical σ bonds but shorter than π bonds; thus, it is appropriate to envisage the Ru(1)—C(2)—Ru(3) bonds at two-electron—three-center (2e—3c) bonds with the C(2) atom donating one electron.

Table 7. Final Atomic Coordinates (Fractional) and B_{eq} Values for 16

atom	x	y	z	B _{eq} , ^a Å ²
Ru(1)	0.130 984(9)	0.169 03(3)	0.045 506(15)	2.53(1)
Ru(2)	0.169 957(9)	0.153 85(3)	0.201 96(2)	2.61(1)
Ru(3)	0.102 646(9)	0.319 22(3)	0.244 41(2)	2.53(1)
Ru(4)	0.067 085(9)	0.344 19(3)	0.082 43(2)	2.52(1)
Ru(5)	0.152 177(9)	0.409 57(3)	0.134 53(2)	2.50(1)
P(1)	0.096 23(3)	0.148 21(9)	0.149 01(5)	2.32(3)
O(1)	0.234 62(11)	0.186 2(4)	0.348 5(2)	6.8(2)
O(2)	0.242 71(9)	0.194 3(3)	0.113 3(2)	4.8(1)
O(3)	0.180 40(12)	-0.146 5(3)	0.231 6(2)	6.7(2)
O(4)	0.084 69(14)	0.613 43(3)	0.272 6(2)	7.8(2)
O(5)	0.159 43(12)	0.319 5(4)	0.399 7(2)	7.6(2)
O(6)	0.032 58(12)	0.219 1(4)	0.328 7(2)	8.2(2)
O(7)	0.010 75(11)	0.561 2(4)	0.135 1(2)	6.8(2)
O(8)	-0.010 14(10)	0.190 4(4)	0.004 3(2)	6.2(2)
O(9)	0.083 55(10)	0.499 1(3)	-0.059 5(2)	5.6(2)
O(10)	0.115 32(11)	0.691 8(3)	0.111 5(2)	6.2(2)
O(11)	0.206 58(11)	0.454 5(4)	0.010 1(2)	6.3(2)
O(12)	0.219 00(11)	0.493 4(4)	0.269 7(2)	7.0(2)
C(1)	0.167 96(13)	-0.001 2(4)	-0.003 3(2)	3.6(2)
C(2)	0.177 32(14)	0.124 5(5)	-0.035 1(2)	4.1(2)
C(3)	0.144 8(2)	0.206 9(4)	-0.073 5(2)	4.3(2)
C(4)	0.102 23(15)	0.168 1(5)	-0.078 9(2)	4.3(2)
C(5)	0.092 22(13)	0.048 6(4)	-0.043 4(2)	3.8(2)
C(6)	0.124 89(14)	-0.035 2(4)	-0.006 6(2)	3.7(2)
C(7)	0.202 3(2)	-0.095 5(5)	0.032 4(3)	5.0(2)
C(8)	0.208 84(13)	0.177 5(5)	0.294 8(2)	4.1(2)
C(9)	0.211 82(14)	0.182 5(4)	0.139 2(2)	4.0(2)
C(10)	0.175 55(14)	-0.033 7(4)	0.220 4(2)	4.0(2)
C(11)	0.090 9(2)	0.503 1(5)	0.259 2(2)	4.7(2)
C(12)	0.140 12(14)	0.313 8(5)	0.338 9(2)	4.6(2)
C(13)	0.058 51(14)	0.255 0(5)	0.295 1(2)	4.6(2)
C(14)	0.032 13(13)	0.478 2(5)	0.117 2(2)	4.2(2)
C(15)	0.018 69(12)	0.248 4(5)	0.034 7(2)	3.9(2)
C(16)	0.078 41(12)	0.438 4(4)	-0.007 2(2)	3.7(2)
C(17)	0.127 65(13)	0.582 7(4)	0.120 0(2)	4.0(2)
C(18)	0.185 38(13)	0.433 9(4)	0.055 3(2)	4.0(2)
C(19)	0.193 73(13)	0.458 1(4)	0.218 9(2)	4.3(2)
C(20)	0.062 26(15)	-0.002 1(4)	0.153 9(2)	4.6(2)
C(21)	0.062 4(2)	-0.064 5(6)	0.228 9(3)	8.4(3)

^a B_{eq} = $\frac{8}{3}\pi^2 \sum \sum U_{ij} a_i^* a_j^* (\mathbf{a}_i \mathbf{a}_j)$.

The structure of this complex is similar to that of 9 except that one carbonyl on Ru(1) is replaced by a phosphine which is attached to the Cp(2) ring.⁸ However, three significant differences should be noted: (1) in complex 9 the ortho-metalated carbon is bonded to two Ru atoms rather unsymmetrically (2.12(2) and 2.45-(2) Å); (2) in complex 9 the Fe—Ru bonding interaction is rather weak, as indicated by the length of 3.097(3) Å, and this bond is even longer than the Ru(1)—Ru(2) bond (3.037(2) Å); (3) in complex 9 there is no bridging or semibridging carbonyl. The presence of the bridging carbonyl C(27)O(1) may be attributed to the strong electron-releasing nature of the Fc groups.

Since the ortho metalation of a Cp ring in forming 11 creates planar chirality, two diastereoisomers are possible for the complex. However, solution NMR spectra, including that of the pyrolysis mixture, reveal only one hydride. There is no obvious explanation for the absence of the other diastereoisomer. Also surprising is the absence of other hydride-containing products from this pyrolysis reaction.

Pyrolysis of the same starting material Ru₃(CO)₁₁(PF₂Ph) in cyclohexane for 6 h, or in toluene for 5 h, affords similar product mixtures, and complex 11 can be isolated in comparable yields.

Pyrolysis of Ru₃(CO)₁₂ and PF₂Ph in a 1:1 molar ratio in octane for 3.5 h affords complex 12 in 12% yield. It shows a ³¹P NMR resonance at 418.0 ppm, suggesting

(17) Clucas, J. A.; Harding, M. M.; Smith, A. K. *J. Chem. Soc., Chem. Commun.* **1985**, 1280.

(18) Osella, D.; Ravera, M.; Smith, A. K.; Mathews, A. J.; Zanello, P. *J. Organomet. Chem.* **1992**, *423*, 255.

(19) Cullen, W. R.; Rettig, S. J.; Zheng, T. C. *Can. J. Chem.* **1992**, *70*, 2329.

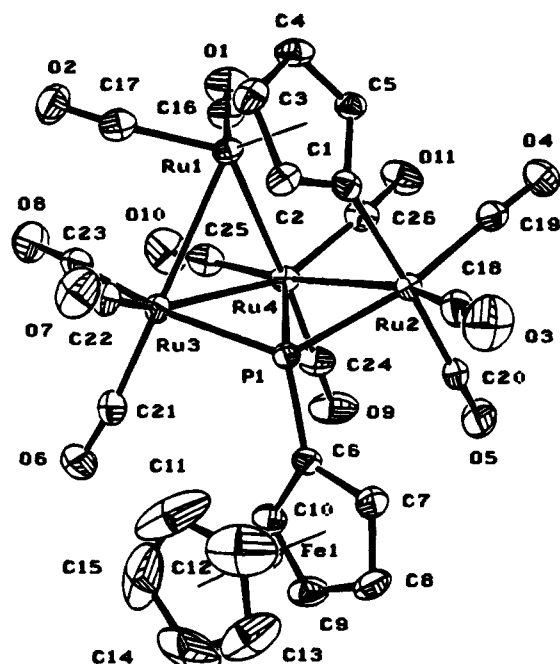


Figure 2. ORTEP diagram for **12** (33% probability thermal ellipsoids).

the presence of a phosphinidene moiety. The ^1H NMR spectrum shows the presence of only 13 ferrocenyl protons, indicating the presence of some unusual features in this complex. The mass spectrum gives the parent ion at m/e 993, corresponding to a formula such as $\text{Ru}_4(\text{CO})_{11}(\text{Pfc})(\text{C}_5\text{H}_4)$. This novel formulation was confirmed by an X-ray diffraction study. An ORTEP diagram with 33% probability thermal ellipsoids is shown in Figure 2.

The metal skeleton of **12** consists of a Ru_3 triangle sharing a Ru—Ru edge with a Ru_3P butterfly arrangement. The $\text{Ru}(1)\text{Ru}(3)\text{Ru}(4)$ plane makes an angle of 75.9° with the $\text{Ru}(2)\text{Ru}(3)\text{Ru}(4)$ plane. The $\text{C}(1)\text{—C}(5)$ Cp ring is σ -bonded to $\text{Ru}(2)$ via $\text{C}(1)$ and π -bonded to $\text{Ru}(1)$. The carbonyl ligands are distributed two to $\text{Ru}(1)$ and three each to $\text{Ru}(2)$, $\text{Ru}(3)$, and $\text{Ru}(4)$, and the whole cluster is electron precise. The $\text{Ru}(1)\text{—Ru}(4)$ bond is the longest at $2.9514(6)$ Å, the $\text{Ru}(1)\text{—Ru}(3)$ and $\text{Ru}(2)\text{—Ru}(4)$ bonds are shorter at $2.8974(7)$ and $2.9199(5)$ Å, respectively, and the $\text{Ru}(3)\text{—Ru}(4)$ bond is the shortest at $2.7874(5)$ Å. The phosphinidene moiety is not symmetrically bound; the $\text{Ru}(4)\text{—P}(1)$ bond ($2.393(1)$ Å) is longer than $\text{Ru}(2)\text{—P}(1)$ ($2.341(1)$ Å), which is longer than $\text{Ru}(3)\text{—P}(1)$ ($2.323(1)$ Å). The $\text{Ru}(2)\text{—C}(1)$ bond at $2.086(4)$ Å is typical of such σ bonds. The $\text{Ru}(1)\text{—C}(\text{Cp}(1))$ distances show some variation, with $\text{Ru}(1)\text{—C}(1)$ and $\text{Ru}(1)\text{—C}(2)$ bonds (average 2.258 Å) being ca. 0.04 Å longer than the other three (average 2.214 Å), and they are longer than the $\text{Fe}\text{—C}$ bonds ($\text{Cp}(2)$ and $\text{Cp}(3)$) (average 2.047 and 2.019 Å), as expected.

The carbonyl $\text{C}\text{—Ru}$ distances show significant variation. The $\text{Ru}(2)\text{—C}(20)$ bond which is trans to the $\text{Ru}(2)\text{—C}(1)$ σ bond is the longest at $1.952(4)$ Å, the $\text{Ru}(2)\text{—C}(19)$ and $\text{Ru}(3)\text{—C}(23)$ bonds which are trans to $\text{Ru}\text{—P}(1)$ bonds average 1.936 Å, the $\text{Ru}(3)\text{—C}(22)$, $\text{Ru}(4)\text{—C}(25)$, and $\text{Ru}(4)\text{—C}(26)$ bonds average 1.913 Å, and the rest average 1.884 Å. The $\text{Ru}\text{—C}\text{—O}$ angles are close to linear only for carbonyls $\text{C}(18)$, $\text{C}(19)$, $\text{C}(22)$, $\text{C}(23)$, and $\text{C}(24)$ (average 117.8°). The rest average to

Table 8. Final Atomic Coordinates (Fractional) and B_{eq} Values for **8**

atom	x	y	z	$B_{\text{eq}}, \text{\AA}^2$
Ru(1)	0.16024(3)	0.29843(6)	0.34285(2)	2.35(1)
Ru(2)	0.36124(3)	0.30064(6)	0.35957(2)	2.40(1)
Ru(3)	0.35125(3)	0.61344(6)	0.38422(2)	2.53(1)
Ru(4)	0.16092(3)	0.61311(6)	0.36864(2)	2.41(1)
Fe(1)	0.22585(7)	0.2320(1)	0.55734(4)	3.09(2)
P(1)	0.2504(1)	0.4136(2)	0.41738(7)	2.18(3)
O(1)	-0.0362(3)	0.3838(7)	0.3173(3)	5.5(2)
O(2)	0.1761(4)	0.0940(7)	0.2362(3)	5.6(2)
O(3)	0.0843(4)	0.0458(7)	0.4193(3)	5.2(2)
O(4)	0.5576(3)	0.4038(7)	0.3629(2)	4.8(1)
O(5)	0.3856(4)	0.0934(8)	0.2549(3)	6.1(2)
O(6)	0.4191(4)	0.0538(7)	0.4467(3)	5.5(2)
O(7)	0.2581(3)	0.9065(6)	0.3618(2)	4.3(1)
O(8)	0.5137(4)	0.7996(8)	0.3525(3)	7.0(2)
O(9)	0.3914(5)	0.7244(7)	0.5072(3)	6.0(2)
O(10)	0.0081(4)	0.7947(8)	0.3138(3)	6.3(2)
O(11)	0.0926(4)	0.7210(6)	0.4841(2)	4.7(1)
C(1)	0.2184(4)	0.4718(6)	0.2940(3)	2.2(1)
C(2)	0.3162(4)	0.4715(7)	0.3015(3)	2.4(1)
C(3)	0.3656(4)	0.5759(8)	0.2703(3)	3.1(2)
C(4)	0.3216(5)	0.6816(8)	0.2332(3)	3.7(2)
C(5)	0.2287(5)	0.6811(8)	0.2260(3)	3.7(2)
C(6)	0.1768(5)	0.5756(8)	0.2555(3)	3.0(2)
C(7)	0.2341(4)	0.3979(7)	0.4946(3)	2.5(1)
C(8)	0.1469(5)	0.3947(8)	0.5217(3)	3.5(2)
C(9)	0.1620(6)	0.4211(9)	0.5827(4)	4.6(2)
C(10)	0.2554(7)	0.434(1)	0.5948(3)	5.1(2)
C(11)	0.3012(5)	0.4156(9)	0.5414(3)	3.7(2)
C(12)	0.2387(5)	0.0214(8)	0.5242(3)	3.9(2)
C(13)	0.1555(5)	0.0349(9)	0.5525(4)	4.3(2)
C(14)	0.1756(6)	0.075(1)	0.6119(4)	5.0(2)
C(15)	0.2711(6)	0.087(1)	0.6204(4)	5.2(2)
C(16)	0.3106(5)	0.051(1)	0.5664(4)	4.7(2)
C(17)	0.0390(5)	0.3612(8)	0.3280(3)	3.3(2)
C(18)	0.1696(5)	0.1696(9)	0.2754(3)	3.5(2)
C(19)	0.1161(4)	0.1388(9)	0.3933(3)	3.3(2)
C(20)	0.4822(4)	0.3748(8)	0.3634(3)	3.2(2)
C(21)	0.3748(5)	0.1707(9)	0.2936(4)	3.8(2)
C(22)	0.3931(5)	0.1446(9)	0.4160(3)	3.5(2)
C(23)	0.2571(4)	0.7788(8)	0.3684(3)	3.0(2)
C(24)	0.4544(5)	0.7251(10)	0.3642(3)	4.1(2)
C(25)	0.3747(5)	0.6797(8)	0.4612(3)	3.6(2)
C(26)	0.0638(5)	0.7235(9)	0.3329(3)	3.4(2)
C(27)	0.1196(4)	0.6766(8)	0.4414(3)	3.1(2)

$$^a B_{\text{eq}} = \frac{8}{3}\pi^2(U_{11}(aa^*)^2 + U_{22}(bb^*)^2 + U_{33}(cc^*)^2 + 2U_{12}aa^*bb^* \cos \gamma + 2U_{13}aa^*cc^* \cos \beta + 2U_{23}bb^*cc^* \cos \alpha).$$

173.4° . The ferrocenyl moiety is unexceptional, and the $\text{Cp}(2)$ and $\text{Cp}(3)$ rings have a small ring tilt angle of 2.8° .

The structure may be compared with that of the (benzyne)chromium tricarbonyl complex $\text{Ru}_3(\text{CO})_9[\text{PC}_6\text{H}_5\text{—Cr}(\text{CO})_3][(\text{C}_6\text{H}_4)\text{Cr}(\text{CO})_3]$ (**18**),²⁰ and it may also be considered as a ruthenium analog of the well-known osmium benzyne complexes $\text{Os}_3(\text{CO})_9(\text{PR})(\text{C}_6\text{H}_4)$ ($\text{R} = \text{Fc}, \text{Ph}, \text{Et}, \text{Me}$).^{1,21–23} The difference between **18** and **12** is that in **18** the $(\text{C}_6\text{H}_4)\text{Cr}(\text{CO})_3$ moiety can be considered to be bound to two Ru centers via two carbon atoms of the C_6H_4 fragment and to the third Ru atom via the chromium atom, while in **12** the $(\text{C}_5\text{H}_4)\text{Ru}(\text{CO})_2$ moiety is bonded to one Ru center via one carbon atom of the C_5H_4 fragment and to the other two Ru centers via the $\text{Ru}(1)$ atom.

(20) Cullen, W. R.; Rettig, S. J.; Zhang, H. *Organometallics* **1991**, *10*, 2965.

(21) Brown, S. C.; Evans, J.; Smart, L. E. *J. Chem. Soc., Chem. Commun.* **1980**, 1021.

(22) Deeming, A. J.; Kabir, S. E.; Powell, N. I.; Bates, P. A.; Hursthouse, M. B. *J. Chem. Soc., Dalton Trans.* **1987**, 1529.

(23) Deeming, A. J.; Marshall, J. E.; Nuel, D.; O'Brien, G.; Powell, N. I. *J. Organomet. Chem.* **1990**, *384*, 347.

Table 9. Selected Bond Lengths (Å) for 11–16 and 8^a

Compound 11			
Ru(1)–Ru(2)	3.0326(3)	Ru(1)–Ru(3)	2.7830(3)
Ru(1)–Fe(1)	2.9866(3)	Ru(1)–C(2)	2.262(2)
Ru(1)–C(27)	1.972(3)	Ru(2)–Ru(3)	2.8882(3)
Ru(2)–P(1)	2.3792(6)	Fe(1)–Cp(1)	1.70
Ru(3)–C(2)	2.249(2)	Fe(2)–Cp(3)	1.64
Fe(1)–C(2)	2.187(2)	Ru(1)–H(1)	1.91(3)
Fe(1)–Cp(2)	1.70	Ru(2)–H(1)	1.74(3)
Fe(2)–Cp(4)	1.66		
Compound 12			
Ru(1)–Ru(3)	2.8974(7)	Ru(2)–P(1)	2.341(1)
Ru(1)–Ru(4)	2.9514(6)	Ru(3)–Ru(4)	2.7874(5)
Ru(1)–Cp(1)	1.876(3)	Ru(3)–P(1)	2.323(1)
Ru(2)–Ru(4)	2.9199(5)	Ru(4)–P(1)	2.393(1)
Compound 13			
Ru(1)–Ru(1)'	2.9606(7)	Ru(3)–Ru(3)'	2.8540(7)
Ru(1)–Ru(2)'	2.9175(4)	Ru(1)–Ru(2)	2.8336(4)
Ru(1)–P(1)	2.2880(9)	Ru(1)–Ru(3)	2.9028(5)
Ru(2)–Ru(3)	2.9025(5)	Ru(2)–Ru(3)'	2.9380(4)
Ru(2)–P(1)	2.2695(9)		
Compound 14			
Ru(1)–Ru(3)	2.8817(6)	Ru(1)–Ru(4)	2.865(1)
Ru(1)–Ru(5)	2.884(1)	Ru(1)–Ru(6)	2.8802(5)
Ru(1)–Cp	1.83	Ru(2)–Ru(3)	2.874(1)
Ru(2)–Ru(4)	2.8825(5)	Ru(2)–Ru(5)	2.8803(6)
Ru(2)–Ru(6)	2.878(1)	Ru(3)–Ru(4)	2.8481(8)
Ru(3)–Ru(6)	2.9600(4)	Ru(3)–P(1)	2.287(1)
Ru(4)–P(1)	2.286(1)	Ru(4)–Ru(5)	2.9314(6)
Ru(5)–Ru(6)	2.8719(8)		
Compound 15			
Ru(1)–Ru(1)*	2.763(2)	Ru(2)–Ru(3)	2.821(2)
Ru(1)–Ru(3)	2.848(1)	Ru(1)–Ru(2)	2.821(1)
Ru(1)–C(1)	2.07(1)	Ru(2)–Ru(2)*	2.896(2)
Ru(1)–Cp	1.86		
Compound 16			
Ru(1)–Ru(2)	2.8250(5)	Ru(2)–Ru(5)	2.8134(6)
Ru(1)–Ru(4)	2.8274(5)	Ru(3)–Ru(4)	2.8922(5)
Ru(1)–Ru(5)	2.8678(6)	Ru(3)–Ru(5)	2.8263(5)
Ru(1)–Cp	1.738	Ru(4)–Ru(5)	2.7902(5)
Ru(2)–Ru(3)	2.8890(5)		
Compound 8			
Ru(1)–Ru(2)	2.9704(8)	Ru(2)–Ru(3)	2.8826(9)
Ru(4)–C(1)	2.306(6)	Ru(2)–C(2)	2.119(6)
Ru(1)–Ru(4)	2.8995(9)	Ru(3)–Ru(4)	2.8122(8)
Ru(1)–C(1)	2.116(6)	Ru(3)–C(2)	2.317(6)

^a Primes refer to the symmetry operation $-x, y, 1/2 - z$, and asterisks refer to the symmetry operation $1 - x, y, z$.

In the formation of complex **12**, the cleavages of one P–Ph bond, one P–Fc bond, and one Fe–Cp π bond, as well as the loss of a phenyl group and a FeCp moiety, have occurred. Ferrocene is typically very resistant to ligand substitution; however, it is known that (C₅H₄-COOH)Fe(C₅H₅) reacts with ⁵⁹FeCl₃ or ¹⁰³RuCl₃ at 180 °C for 2 h in an evacuated tube to afford radiolabeled metallocene carboxylic acids.²⁴ In the present study, however, the cleavage reaction occurred under rather mild conditions (125 °C, 1 atm, 3.5 h). It is certainly an unprecedented reaction.

Compound **8** was originally obtained in low yield (2%) by heating Ru₃(CO)₁₀Fc'(PPh₂)₂ in cyclohexane for 2 h. It was one of about 18 products.⁸ In the present work the compound was isolated in 10% yield from Ru₃(CO)₁₁-PFc₂Ph (refluxing hexanes, 15 h), and in 20% yield by reacting Ru₃(CO)₁₂ with PFc₂Ph in refluxing cyclohexane (1 h). Related benzyne derivatives with μ_4 -phosphinidene groups (μ_4 -PR) are obtained by heating Ru₃(CO)₁₁PPh₂R (R = Ph, Me, CH₂NPh₂).²⁵

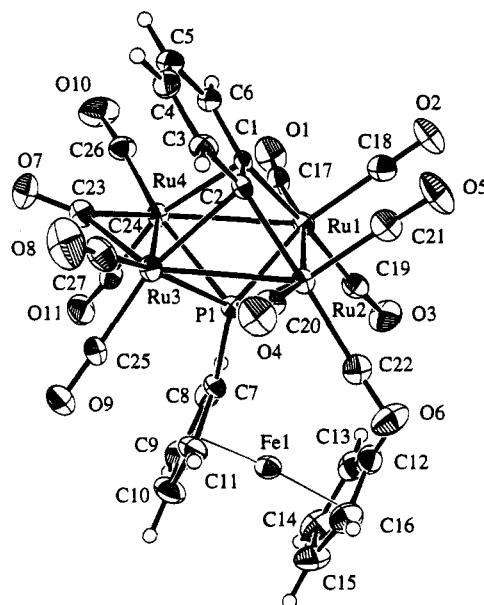


Figure 3. ORTEP diagram for **8** (33% probability thermal ellipsoids).

In the redetermined structure of **8** (Figure 3), (new *R* value 0.042, old *R* value 0.114), the bond angles and distances are much closer to those of the two other known structures of this type (PR = Ph, CH₂NPh₂).²⁵ For example, Ru(1)–Ru(2), bridged by CO, is now the shortest metal–metal bond in **8** at 2.8122(8) Å and the dihedral angle between the benzyne and the Ru₄ plane is 51.1°. When PR = PCH₂NPh₂, the corresponding values are 2.816(1) Å and 50.9°. The benzyne moiety acts as a six-electron donor via two σ bonds and two asymmetric η^2 bonds involving C(2)C(3) and C(1)C(6), and as a consequence, Ru(2)–C(2) (2.119(6) Å) is shorter than Ru(3)–C(2) (2.317(6) Å), which is shorter than Ru(3)–C(3) (2.625(7) Å). The corresponding distances when PR = PCH₂NPh₂ are 2.117(3), 2.301(4), and 2.634(4) Å. The C(1)–C(2) bond distance is elongated to 1.444(6) Å, and C(4)–C(5) may be shortened (1.37(1) Å) because of electron localization.

Pyrolysis of Ru₃(CO)₁₂ with PET₂Fc. Pyrolysis of Ru₃(CO)₁₂ with PET₂Fc in octane for 18 h affords complexes **13** and **14** in 15% and 25% yields, respectively, and **15** in low yield.

Complex **13** shows a ³¹P NMR resonance at 370.4 ppm, suggesting the presence of a phosphinidene/phosphido moiety. The ¹H NMR spectrum shows the presence of only ethyl protons. The number of protons could not be established with certainty. The mass spectrum gives the parent ion at *m/e* 1189, corresponding to a formula such as Ru₆C(CO)₁₄(PET₂)₂. The structure was determined by using X-ray crystallography. An ORTEP diagram with 33.0% probability thermal ellipsoids is shown in Figure 4.

The structure of complex **13** consists of a slightly distorted hexaruthenium octahedron with an interstitial carbon atom at the center of the octahedron. The molecule has crystallographic C₂ symmetry. The Ru(1)–Ru(2) bond is the shortest at 2.8336(4) Å and is bridged symmetrically by the phosphido moiety PET₂

(25) Knox, S. A. R.; Lloyd, B. R.; Morton, D. A. V.; Nicholls, S. M.; Orpen, A. G.; Vinas, J. M.; Weber, M.; Williams, G. K. *J. Organomet. Chem.* **1990**, 394, 385.

(24) Wenzel, M.; Nipper, E.; Klose, W. *J. Nucl. Med.* **1977**, 18, 367.

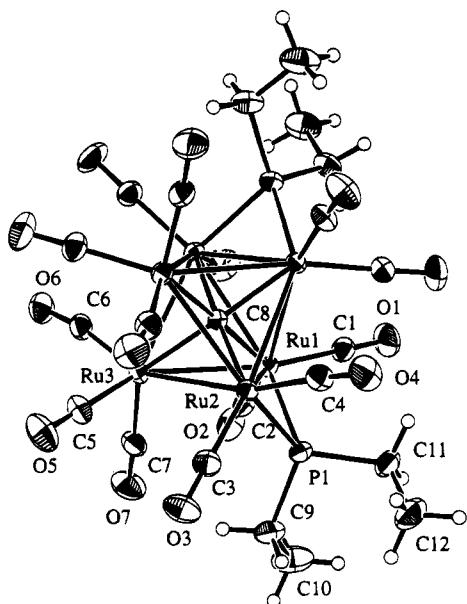


Figure 4. ORTEP diagram for **13** (33% probability thermal ellipsoids).

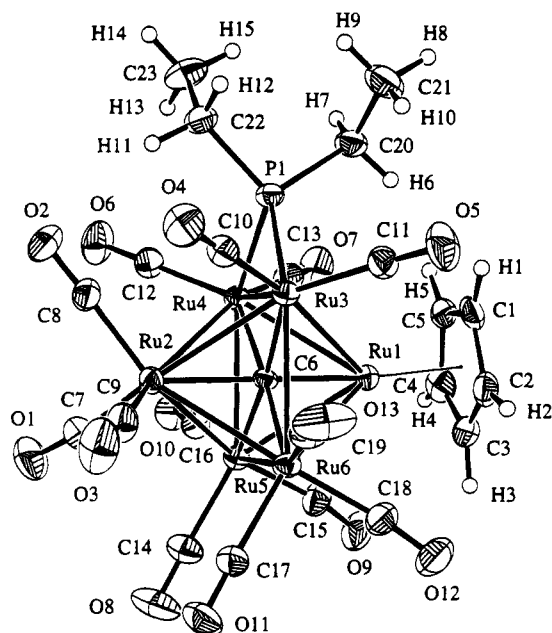


Figure 5. ORTEP diagram for **14** (33% probability thermal ellipsoids).

(2.2695(9) and 2.2880(9) Å). The Ru(1)–Ru(3) (2.9028(5) Å) and Ru(2)–Ru(3) (2.9025(5) Å) bonds are equal. The Ru(1)–Ru(1') bond at 2.9606(7) Å is the longest. The carbide carbon atom C(8) is bound to Ru atoms equally (average 2.051 Å). The P(1) atom is only 0.13 Å away from the Ru(1)Ru(2)C(8) plane. The Ru–C(carbonyl) distances range from 1.871(4) to 1.925(4) Å. The Ru(3)–C(6)–O(6) angle is 169.2(3)°, much smaller than the rest, which average to 177.7°.

In the formation of complex **13**, two P–Fc bonds have been cleaved and the ferrocenyl moieties lost. Clearly the ferrocenyl C–H metalation reaction is not a facile process such as observed with Os₃ cluster systems;^{1–6} apparently ferrocenyl C–P bonds are much more readily cleaved than ethyl C–P bonds.

Complex **14** shows a ³¹P NMR resonance at 366.8 ppm, again suggesting the presence of a phosphinidene/

Table 10. Selected Bond Angles (deg) for **11–16** and **8^a**

Compound 11			
Ru(2)–Ru(1)–Ru(3)	59.369(8)	Ru(2)–Ru(1)–Fe(1)	100.691(10)
Ru(3)–Ru(1)–Fe(1)	98.42(1)	Ru(1)–Ru(2)–Ru(3)	56.009(6)
Ru(1)–Ru(3)–Ru(2)	64.621(8)		
Compound 12			
Ru(3)–Ru(1)–Ru(4)	56.92(1)	Ru(1)–Ru(4)–Ru(2)	80.56(1)
Ru(4)–Ru(2)–P(1)	52.74(3)	Ru(1)–Ru(4)–Ru(3)	60.57(2)
Ru(1)–Ru(3)–Ru(4)	62.52(1)	Ru(2)–Ru(4)–Ru(3)	95.57(1)
Compound 13			
Ru(1')–Ru(1)–Ru(2)	60.419(9)	Ru(1')–Ru(2)–Ru(3)	89.79(1)
Ru(1')–Ru(1)–Ru(3)	88.940(8)	Ru(3)–Ru(2)–Ru(3')	58.50(1)
Ru(2)–Ru(1)–Ru(3)	60.78(1)	Ru(1)–Ru(3)–Ru(2)	58.43(1)
Ru(1)–Ru(2)–Ru(1')	61.95(1)	Ru(1)–Ru(3)–Ru(3')	91.046(8)
Ru(1)–Ru(2)–Ru(3')	90.73(1)	Ru(2)–Ru(3)–Ru(3')	61.373(10)
Ru(1')–Ru(2)–Ru(3')	59.44(1)	Ru(1)–P(1)–Ru(2)	76.89(3)
Ru(1')–Ru(1)–Ru(2')	57.63(1)	Ru(1)–Ru(3)–Ru(2')	59.93(1)
Ru(2)–Ru(1)–Ru(2')	90.55(1)	Ru(2)–Ru(3)–Ru(2')	88.80(1)
Ru(2')–Ru(1)–Ru(3)	60.63(1)	Ru(2')–Ru(3)–Ru(3')	60.13(1)
Ru(1)–Ru(2)–Ru(3)	60.79(1)		
Compound 14			
Ru(3)–Ru(1)–Ru(4)	59.42(1)	Ru(2)–Ru(4)–Ru(3)	60.19(2)
Ru(3)–Ru(1)–Ru(6)	61.82(1)	Ru(3)–Ru(4)–Ru(5)	90.66(2)
Ru(4)–Ru(1)–Ru(6)	91.09(2)	Ru(2)–Ru(3)–Ru(6)	59.10(2)
Ru(3)–Ru(2)–Ru(5)	91.18(2)	Ru(1)–Ru(4)–Ru(2)	89.17(2)
Ru(4)–Ru(2)–Ru(5)	61.15(1)	Ru(1)–Ru(4)–Ru(5)	59.66(2)
Ru(5)–Ru(2)–Ru(6)	59.83(1)	Ru(2)–Ru(4)–Ru(5)	59.39(1)
Ru(1)–Ru(3)–Ru(4)	60.00(2)	Ru(1)–Ru(5)–Ru(4)	59.02(2)
Ru(3)–Ru(1)–Ru(5)	90.95(2)	Ru(2)–Ru(5)–Ru(4)	59.46(1)
Ru(4)–Ru(1)–Ru(5)	61.32(3)	Ru(4)–Ru(5)–Ru(6)	89.91(2)
Ru(5)–Ru(1)–Ru(6)	59.77(1)	Ru(1)–Ru(6)–Ru(3)	59.11(1)
Ru(3)–Ru(2)–Ru(4)	59.31(1)	Ru(3)–Ru(6)–Ru(3)	58.96(2)
Ru(3)–Ru(2)–Ru(6)	61.95(3)	Ru(3)–Ru(6)–Ru(5)	89.62(2)
Ru(4)–Ru(2)–Ru(6)	90.78(2)	Ru(1)–Ru(5)–Ru(2)	88.84(1)
Ru(1)–Ru(3)–Ru(2)	89.02(2)	Ru(1)–Ru(5)–Ru(6)	60.05(2)
Ru(1)–Ru(3)–Ru(6)	59.06(1)	Ru(2)–Ru(5)–Ru(6)	60.04(2)
Ru(2)–Ru(3)–Ru(4)	60.50(2)	Ru(1)–Ru(6)–Ru(2)	88.96(2)
Ru(4)–Ru(3)–Ru(6)	89.81(2)	Ru(1)–Ru(6)–Ru(5)	60.18(2)
Ru(1)–Ru(4)–Ru(3)	60.58(2)	Ru(2)–Ru(6)–Ru(5)	60.13(2)
Compound 15			
Ru(1)–Ru(1)–Ru(2)	91.35(2)	Ru(1)*–Ru(1)–Ru(3)	60.98(2)
Ru(1)–Ru(2)–Ru(3)	60.63(4)	Ru(2)–Ru(1)–Ru(3)	59.69(4)
Ru(1)–Ru(3)–Ru(1)	58.04(4)	Ru(1)–Ru(2)–Ru(2)*	88.65(2)
Ru(1)–Ru(3)–Ru(2)*	89.61(5)	Ru(2)*–Ru(2)–Ru(3)	59.12(2)
Ru(2)–Ru(3)–Ru(2)*	61.77(4)	Ru(1)–Ru(3)–Ru(2)	59.68(4)
Compound 16			
Ru(2)–Ru(1)–Ru(4)	91.66(1)	Ru(2)–Ru(5)–Ru(3)	61.63(1)
Ru(2)–Ru(1)–Ru(5)	59.23(1)	Ru(2)–Ru(5)–Ru(4)	92.69(1)
Ru(4)–Ru(1)–Ru(5)	58.67(1)	Ru(3)–Ru(5)–Ru(4)	61.98(1)
Ru(1)–Ru(2)–Ru(3)	89.61(1)	Ru(2)–Ru(3)–Ru(4)	89.00(1)
Ru(1)–Ru(2)–Ru(5)	61.14(1)	Ru(2)–Ru(3)–Ru(5)	58.97(1)
Ru(3)–Ru(2)–Ru(5)	59.41(1)	Ru(4)–Ru(3)–Ru(5)	58.39(1)
Ru(1)–Ru(5)–Ru(2)	59.63(2)	Ru(1)–Ru(4)–Ru(3)	89.50(1)
Ru(1)–Ru(5)–Ru(3)	90.01(1)	Ru(1)–Ru(4)–Ru(5)	61.39(1)
Ru(1)–Ru(5)–Ru(4)	59.94(1)	Ru(3)–Ru(4)–Ru(5)	59.62(1)
Compound 8			
Ru(2)–Ru(1)–Ru(4)	88.36(2)	Ru(1)–Ru(2)–Ru(3)	88.50(2)
Ru(2)–Ru(3)–Ru(4)	91.84(2)	Ru(1)–Ru(4)–Ru(3)	91.30(2)

^a Primes refer to the symmetry operation $-x, y, 1/2 - z$, and asterisks refer to the symmetry operation $1 - x, y, z$.

phosphido moiety. The ¹H NMR spectrum indicates the presence of two ethyl groups and one C₅H₅ ring. The mass spectrum gives the parent ion at *m/e* 1137, corresponding to a formula such as Ru₆C(CO)₁₃(C₅H₅)-(PET₂). The structure of this complex was determined by an X-ray diffraction study. An ORTEP diagram with 33% probability thermal ellipsoids is shown in Figure 5.

The structure of complex **14** is very similar to that of **13** discussed above, but only the Ru(3)–Ru(4) edge is bridged by the phosphido moiety PET₂. The Ru(1) atom is η⁷-bonded to a C₅H₅ ring which is derived from a ferrocenyl moiety. The Ru(2), Ru(5), and Ru(6) atoms

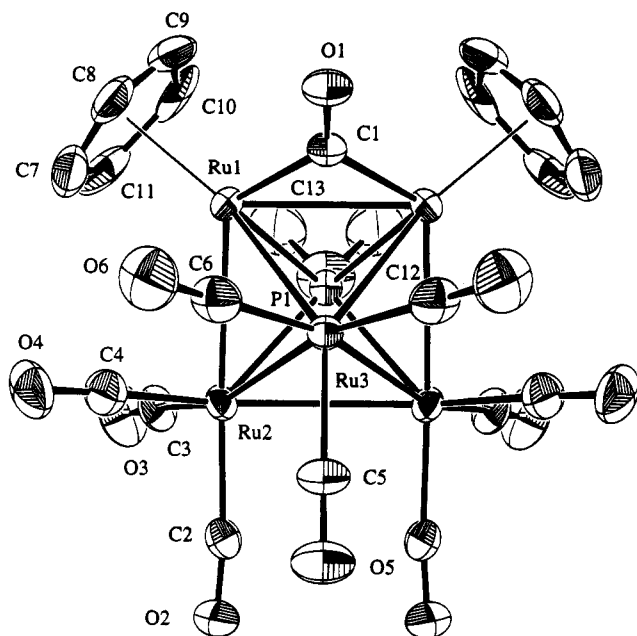


Figure 6. ORTEP diagram for **15** (33% probability thermal ellipsoids).

are each bonded to three CO groups and the Ru(3) and Ru(4) atoms to two. The Ru(3)–Ru(6) and Ru(4)–Ru(5) bonds are the longest at 2.9600(4) and 2.9314(4) Å, respectively, and the CO-bridged Ru(3)–Ru(4) bond at 2.8481(8) Å is the shortest; the rest average to 2.8775 Å. The carbide carbon atom C(6) is bonded to Ru(3), Ru(4), Ru(5), and Ru(6) equidistantly (average 2.055 Å) as for **13**, while C(6)–Ru(1) at 1.933(4) Å is ca. 0.12 Å shorter and C(6)–Ru(2) at 2.101(4) Å is slightly longer. P(1) is symmetrically bonded to the Ru(3) and Ru(4) atoms (2.287(1) and 2.286(1) Å), and it is only 0.18 Å away from the Ru(3)Ru(4)Ru(5)Ru(6) plane. The Ru(1)–C(Cp(1)) distances average to 2.184 Å, comparable to those in **12**. The Ru–C(carbonyl) distances vary little, ranging from 1.869(4) to 1.916(4) Å with an average of 1.895 Å. The Ru–C–O angles for Ru(2)–C(7)–O(1), Ru(5)–C(15)–O(9), Ru(5)–C(16)–O(10), Ru(6)–C(18)–O(12), and Ru(6)–C(19)–O(13) (average 171.7°) are somewhat smaller than the rest, which have an average of 177.3°.

In the formation of complex **14**, one P–Fc bond has been cleaved, as in the formation of **13** from the same reaction. More interestingly, the ferrocenyl moiety is only partially lost, and a C₅ moiety has transferred to Ru(1). This is similar to the reaction resulting in the formation of **12**; however, in **12** it is presumably the C₅H₄ ring that is retained, while in **14** it is unclear whether the C₅H₅ ring is derived from a C₅H₅ or C₅H₄ ring of the ferrocenyl group. If the latter is the case, the extra proton presumably comes from the solvent.

Compounds **13** and **14** belong to a well-known class of ruthenium carbido cluster complexes,²⁶ which includes the parent compound²⁷ Ru₆C(CO)₁₇ and some derivatives such as Ru₆C(CO)₁₄(NO)₂,²⁸ Ru₆C(CO)₁₅–

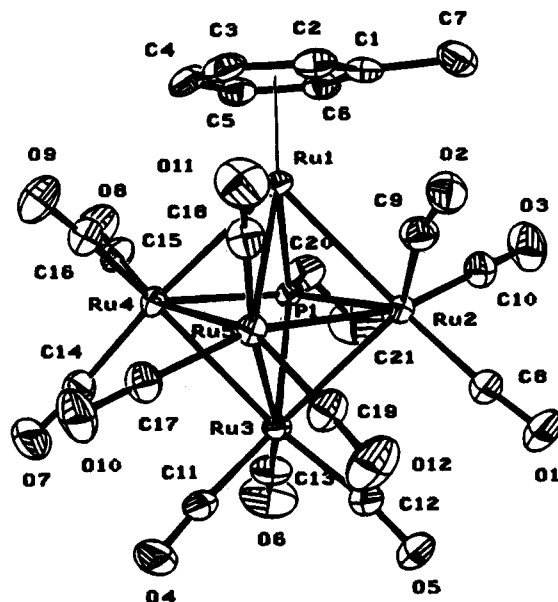


Figure 7. ORTEP diagram for **16** (33% probability thermal ellipsoids).

(NO)(AuPPh₃),²⁸ Ru₆C(CO)₁₄(1,3,5-C₆H₃Me₃),²⁹ Ru₆C(CO)₁₆(PEtPh₂),³⁰ and Ru₆C(CO)₁₆[Cu(MeCN)]₂.³¹ However, we know of no derivatives of such carbido clusters containing two phosphido moieties or one phosphido moiety and a Cp ring.

The structure of the other product, **15**, is shown in Figure 6. The basic skeleton consists of a Ru₅P octahedron. The molecule has crystallographic mirror symmetry with the β-carbon of the P-ethyl group being disordered. The presence of two C₅H₅ groups η⁵ bound to Ru(1) and Ru(2) indicates that at least two molecules of PET₂Fc were involved in the formation of **15**. The cleavage of a P–Et bond is noteworthy. These observations probably account for the low yields of the compound. The CO-bridged Ru–Ru bond at 2.763(2) Å is shorter than the corresponding bond in **8** (2.8122(8) Å). The Ru–Cp distance at 1.86 Å is comparable to that in **14** (1.83 Å).

Pyrolysis of Ru₃(CO)₁₂ with PET₂Fc₂. Pyrolysis of Ru₃(CO)₁₂ with PET₂Fc₂ in toluene for 10 h affords complex **16** in ~5% yield. This was the only product, of many, that was isolated as a pure material. It shows a ³¹P NMR resonance at 425.1 ppm, suggesting the presence of a phosphinidene moiety. The mass spectrum gives the parent ion at *m/e* 995, corresponding to a formula such as Ru₅(CO)₁₂(PET)(C₇H₈). An X-ray diffraction study was carried out to establish the structure, and an ORTEP diagram of **16** with 33% probability thermal ellipsoids is shown in Figure 7.

The molecular structure of **16** consists of a Ru₅P octahedron with an Et group on phosphorus and a η⁶-coordinated toluene molecule on a neighboring Ru atom. The other four Ru atoms are each coordinated to three carbonyls. The octahedron is very regular; for example, the angle between the Ru(1)Ru(3)Ru(4) and Ru(1)Ru(3)Ru(5)P(1) planes is 89.5°. The Ru–Ru bond lengths vary slightly from 2.7902(5) to 2.8922(5) Å. The

(26) Johnson, B. F. G.; Lewis, J.; Nelson, W. J. H.; Nicholls, J. N.; Vargas, M. D. *J. Organomet. Chem.* **1983**, *249*, 255.

(27) Sirigu, A.; Bianchi, M.; Benedetti, E. *J. Chem. Soc. D* **1969**, 596.

(28) Braga, D.; Clegg, W.; Johnson, B. F. G.; Lewis, J.; McPartlin, M.; Nelson, W. J. H.; Puga, J.; Raithby, P. R. *J. Organomet. Chem.* **1983**, *243*, C13.

(29) Mason, R.; Robinson, W. R. *J. Chem. Soc. D* **1968**, 468.

(30) Brown, S. C.; Evans, J.; Webster, M. *J. Chem. Soc., Dalton Trans.* **1981**, 2263.

(31) Bradley, J. S.; Pruet, R. L.; Hill, E.; Ansell, G. B.; Leonowicz, M. E.; Modrick, M. A. *Organometallics* **1982**, *1*, 748.

phosphinidene bridge is unsymmetrical with the P(1)–Ru(1) bond (2.2836(9) Å) being the shortest, P(1)–Ru(2) and P(1)–Ru(4) the longest (average 2.378 Å), and P(1)–Ru(3) intermediate at 2.3659(9) Å. The toluene moiety is η^6 -bonded to Ru(1), although the Ru(1)–C(1) distance at 2.300(4) Å is significantly longer than the others due to the steric interaction between the Me group on C(1) and the carbonyl C(9)–O(2) on Ru(2). This interaction is reflected in the bending of the carbonyl (167.1(4)°) and in the slight bending of the Me group away from the C(1)–C(6) plane (0.111 Å). The Ru(1)–C(5) bond at 2.180(4) Å is slightly shorter than the other four (average 2.230 Å). The structure of complex **16** is very closely related to that of $\text{Ru}_5(\text{CO})_{15}(\mu_4\text{-Pr})$ (R = Me, Et, Ph, Bz)³² or $\text{Os}_5(\text{CO})_{15}[\mu_4\text{-P(OMe)}]$.³³ The interesting feature is the bonding of the toluene molecule to the Ru atom, although other examples involving η^6 -arenes are known: $(\eta^6\text{-C}_6\text{H}_6)\text{Ru}(\text{MeC}\equiv\text{CMe})\text{Os}_3(\text{CO})_9$,³⁴ $\text{Ru}_6\text{C}(\text{CO})_{11}(\eta^6\text{-1,3,5-C}_6\text{H}_3\text{Me}_3)(\eta^6\text{-C}_6\text{H}_6)$,³⁵ and $\text{Ru}_6\text{C}(\text{CO})_{11}(\eta^6\text{-1,3,5-C}_6\text{H}_3\text{Me}_3)_2$.³⁵

The formation of complex **16** apparently involves

(32) Natarajan, K.; Zsolnai, L.; Huttner, G. *J. Organomet. Chem.* **1981**, *209*, 85.

(33) Fernandez, J. M.; Johnson, B. F. G.; Lewis, J.; Raithby, P. R. *J. Chem. Soc., Chem. Commun.* **1978**, 1015.

many steps, but two pertinent features are (1) a toluene molecule is incorporated into the complex from the solvent and (2) two ferrocenyl groups in PEtFc_2 are lost via two ferrocenyl C–P bond cleavages. It is not clear whether they are lost as ferrocene or as biferrocenyl, but the preferred P–Fc cleavage over P–Et cleavage is similar to that discussed above.

Acknowledgment. We thank the Natural Sciences and Engineering Research Council of Canada for support of this work (W.R.C.) and the University of British Columbia for a graduate fellowship (T.C.Z.).

Supplementary Material Available: Tables of anisotropic thermal parameters, bond lengths, bond angles, torsion angles, intermolecular contacts, and least-squares planes for all seven structures and of hydrogen parameters for **8** and **11–15** (132 pages). Ordering information is given on any current masthead page. Structure factor listings are available from the authors.

OM940230K

(34) Brooker, A. T.; Jackson, P. A.; Johnson, B. F. G.; Lewis, J.; Raithby, P. R. *J. Chem. Soc., Dalton Trans.* **1991**, 707.

(35) Braga, D.; Grepioni, F.; Righi, S.; Dyson, P. J.; Johnson, B. F. G.; Bailey, P. J.; Lewis, J. *Organometallics* **1992**, *11*, 4042.